

See discussions, stats, and author profiles for this publication at: <https://www.researchgate.net/publication/330029510>

Local Thermophysical Properties Measurements on Polymers using Doped Silicon SThM Probe: Uncertainty Analysis and Interlaboratory Comparison

Conference Paper · September 2018

DOI: 10.1109/THERMINIC.2018.8593308

CITATIONS

0

READS

30

11 authors, including:



Guen Eloise

Institut National des Sciences Appliquées de Lyon

2 PUBLICATIONS 1 CITATION

[SEE PROFILE](#)



Petr Klapetek

Czech Metrology Institute

118 PUBLICATIONS 1,986 CITATIONS

[SEE PROFILE](#)



Robert Puttock

National Physical Laboratory

11 PUBLICATIONS 32 CITATIONS

[SEE PROFILE](#)



B. Hay

Laboratoire National de Métrologie et d'Essais

97 PUBLICATIONS 572 CITATIONS

[SEE PROFILE](#)

Some of the authors of this publication are also working on these related projects:



Measurement uncertainty software [View project](#)



Conformity assessment [View project](#)

Local Thermophysical Properties Measurements on Polymers using Doped Silicon SThM Probe: Uncertainty Analysis and Interlaboratory Comparison

Eloïse Guen¹, Pierre-Olivier Chapuis¹, Petr Klapetek^{2,3}, Robb Puttock⁴, Bruno Hay⁵, Alexandre Allard⁵, Tony Maxwell⁴, David Renahy⁶, Miroslav Valtr³, Jan Martinek² and Séverine Gomès^{1*},

¹ CETHIL UMR5008, Univ Lyon, CNRS, INSA-Lyon, Université Claude Bernard Lyon 1, F-69621, Villeurbanne, France

² Czech Metrology Institute, Okružní 31, 638 00 Brno, Czech Republic

³ CEITEC, Brno University of Technology, Purkyňova 123, 612 00 Brno, Czech Republic

⁴ National Physical Laboratory (NPL), Queens Road, Teddington, Middlesex TW11 0LW, UK

⁵ Laboratoire National de métrologie et d'Essais (LNE), 29 avenue Roger Hennequin, 78197 Trappes Cedex, France

⁶ ILM UMR5008, Univ Lyon, CNRS, INSA-Lyon, Université Claude Bernard Lyon 1, F-69621, Villeurbanne, France

* Corresponding Author: severine.gomes@insa-lyon.fr, +33 47243 6428

Abstract

We first assess Scanning Thermal Microscopy (SThM) with a self-heated doped silicon nanoprobe as a method for the simultaneous identification of the local thermal conductivity and phase transition temperature of polymeric materials. In a second step, results of an interlaboratory comparison and an uncertainty analysis involving three laboratories applying the same protocol of phase transition temperature measurement allow evaluating the repeatability, the reproducibility and the reliability of the method.

1. Introduction

The manufacturing industry and microelectronics have acknowledged a strong need to develop methodologies to characterise polymeric-based composite materials in a spatially resolved manner, in particular thermal interface materials. However, at present there is a scarcity of such methodologies. Local analysis may be addressed by techniques involving interface spectroscopic or mechanical measurements with some forms of microscopy such as atomic force microscopy (AFM), Raman microscopy or near-infrared microscopy. In this study, we analyse the use of scanning thermal microscopy (SThM, see Figure 1) [1] as a means of local thermal measurements.

In first step, we explore SThM for the simultaneous identification of the thermal conductivity and phase transition temperature (glass transition temperature, T_g and melting temperature, T_m) of polymeric materials. In a second step, we report the results of an interlaboratory comparison between three laboratories applying the same protocol of measurement to determine the phase transition temperature of polymers. This allows evaluating the repeatability, the reproducibility and the reliability of the method.

2. Samples and setups

2.1 Principle of the measurements

The principle is to perform an analysis of the AFM probe deflection while it is progressively heated (see Figure 2a) by means of a thermoresistive heater, which acts also as a temperature sensor [1] and is located on the top side of the cantilever of the AM probe. The tip is therefore made of a pyramidal shape of 5 micron height (see Figure 1b).

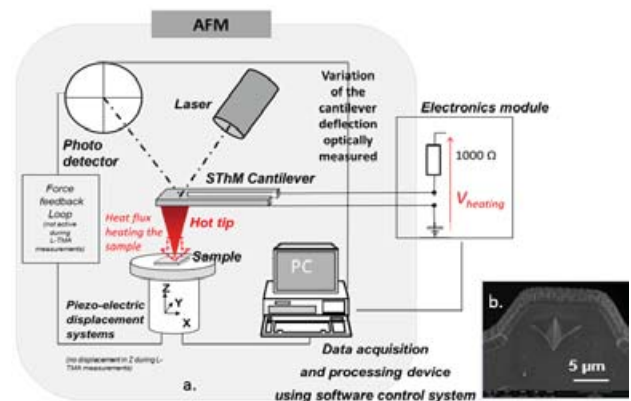


Figure 1: (a) SThM setup and (b) SEM image of a doped silicon probe.

2.2 Samples

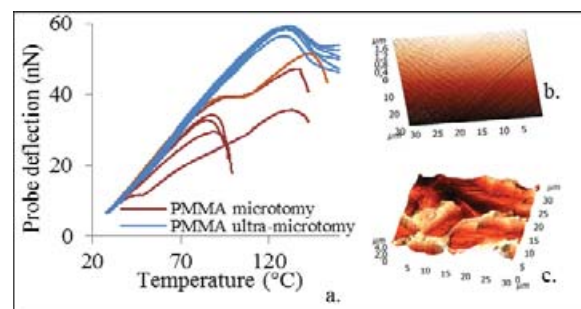


Figure 2: (a) Thermomechanical measurements of PMMA samples for two types of surfaces. (b,c) Topography images obtained by AFM of a PMMA sample surface prepared using (b) ultra-microtomy and (c) usual microtomy.

Samples consist of nine reference bulk samples with phase transition temperature (Table 1) measured using differential scanning calorimetry (DSC) [2]. In the interlaboratory comparison semi-crystalline materials were used as calibration samples and amorphous polymers as test samples. Their surfaces were prepared using *ultra-microtomy*. As shown in Figure 2(b,c), this ensures a much better reproducibility of the measurement and strongly reduces the artefact of topography on the measurement that can be observed when the studied surfaces are prepared using standard *microtomy*. R_q roughness of each samples was measured using AFM in intermittent contact mode and was found between 10 and 20 nm depending on the specimen.

Table 1: Phase transition temperature and thermal conductivity of the studied reference bulk samples [2].

Polymeric material		DSC T (°C) ⁽ⁱ⁾	Thermal conductivity (W.m ⁻¹ .K ⁻¹)
Amorphous polymers	Polyvinylchloride (PVC)	65.2	0.238 ⁽ⁱⁱ⁾
	Polystyrene (PS)	118.0	0.2 ⁽ⁱⁱⁱ⁾
	Polymethyl methacrylate (PMMA)	120.1	0.33 ⁽ⁱⁱⁱ⁾
	Polycarbonate (PC)	148.8	0.22-0.24 ⁽ⁱⁱⁱ⁾
	Polysulfone (PSu)	187.0	0.265 ⁽ⁱⁱ⁾
Semi-crystalline polymers	Polycaprolactone (PCL)	61.7	0.2 ⁽ⁱ⁾
	Low Density Polyethylene (LDPE)	110.4	0.33 ⁽ⁱⁱⁱ⁾
	Polyoxymethylene (POM)	166.9	0.22-0.24 ⁽ⁱⁱⁱ⁾
	Polyethylene terephthalate (PET)	249.3	0.265 ⁽ⁱⁱ⁾

⁽ⁱ⁾ The expanded uncertainty associated to the determination of phase change temperatures is estimated between 1.2 K and 2.5 K except for PVC where it is of 7 K.

⁽ⁱⁱ⁾ The expanded uncertainty associated to the determination of thermal conductivity at 23 °C is estimated to 5 %.

⁽ⁱⁱⁱ⁾ From provider.

2.3 Setups

Three different SThM devices (Table 2) were used for the interlaboratory comparison. All these devices comprise four main components (as shown in Figure 1): an AFM using a laser-detection system of the motion of the cantilever, a doped silicon SThM nanotip (DS probe supplied by Bruker or Anasys Instruments) [1,3], an electronics module and a software control system. The electronics module allows the electrical heating of the probe, measuring the voltage applied to the probe and the probe electrical resistance R_p .

All the experiments of this study were performed under ambient air conditions.

Table 2: SThM setups.

Device code	AFM	SThM probe	Electronics module and software control system
Device 1	Dimension Icon microscope (Bruker)	VITA-NANOTA-200&300	Developed in CMI
Device 2	NTEGRA-Aura microscope (NT-MDT)	VITA-NANOTA-300	NanoTa module from Anasys Instruments
Device 3	NanoIR2-s by Anasys Instruments	PR-EX-AN2-200	NanoTa module and software from Anasys Instruments

Note that silicon substrate was systematically measured between the measurements of polymeric specimens to estimate the thermal drift in the measurement set (additionally to the probe thermomechanical measurement for the probe free in air) and to regularly verify if polymer residues contaminate the probe. For such highly diffusive material the heat amount transferred from the hot tip to the sample strongly depends on the thermal resistance at the probe-sample contact. Any variation in the signals measured on the silicon sample allow detecting a change at the tip apex that can affect a measurement set.

3. Simultaneous analysis of thermal conductivity and phase change temperature

Thermophysical property measurements, i.e. thermal conductivity and phase transition temperature measurements, were performed with the DS probe. For such measurements the variation of the power electrically dissipated in the probe, P , is measured while the DS probe is heated with a current ramp. This can be done for various probe temperatures T_p .

3.1 Calibration in temperature

The performed phase transition measurements follow the experimental steps suggested by Anasys Instruments [3-4] but as previously described here the probe was not calibrated in temperature using polymeric samples of well-known melting temperature.

For our study T_p is deduced from the probe calibration in an oven, keeping in mind that the probe is not isothermal while heated by joule effect, whether in contact with a sample or far from it. Calibrations using polymeric samples of well-known melting temperature are described in Section 4 of this paper. We will then compare the results obtained using both the used calibration methods.

Note that only one setup, Device 2, is used in this Section, and not all three setups.

3.2 Calibration in thermal conductivity

A calibration curve of the power (thermal conductance) dissipated from the probe to various samples was first determined. We assume that $P = f(T_p)$ is almost linear in the temperature range reached during the current ramp, the slope dP/dT_p provides then the global thermal conductance of the probe-sample system, G_{tot} . Measurement of G_{tot} while the probe is in contact with the samples (ic) or far from them (f) allow to calibrate the probe for thermal conductivity measurement using reference samples of well-known thermal, mechanical and roughness properties [2]. Figure 3 gives the results of such calibration for a DS probe. The signal $S_{thermal} = (G_{tot_ic\ sample} - G_{tot_f\ sample}) / (G_{tot_ic\ Si} - G_{tot_f\ Si})$ is plotted as a function of the thermal conductivity of sample. This normalization allows removing the effect of the long-time thermal drift. It is important to note that the experimental uncertainty in the signal $S_{thermal}$ is much smaller than actual size of the dots plotted. Results demonstrate a range of sensitivity in thermal conductivity for thermal conductivity up to $\sim 3 \text{ W.m}^{-1}.\text{K}^{-1}$, compatible with polymers. The deviation of the experimental data from the curve (fit) observed in this range of thermal conductivities is an indication that nanoprobe are also strongly sensitive to other parameters than thermal conductivity, i.e. various tip-sample contact physical parameters such as roughness, thermal boundary resistance, surface state.

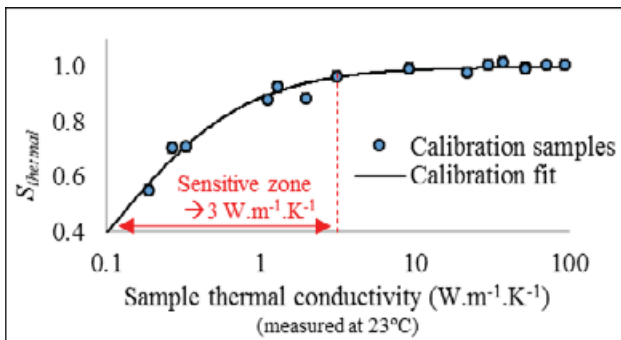


Figure 3: Calibration of a DS probe for thermal conductivity measurement.

3.3 Measurement procedure

After switching off the AFM microscope feedback while keeping the probe-sample contact the deflection of the cantilever is measured as a function of T_p (see an example of thermomechanical measurements on the PMMA sample in Figure 1). The phase transition temperature can be determined from the maximum or the inflection point of the curve of the cantilever deflection as a function of T_p . In the cases of local melting of a semi-crystalline polymer or local softening of an amorphous polymer the transition temperature is the point in the curve right before the probe starts to get immersed inside the sample which gets softer. Here, the power P dissipated in the probe were measured simultaneously to the cantilever deflection, so that dP/dT_p and G_{global} can also be determined as a function of T_p .

3.4 Results and discussion

As an example, Figure 4 gives data measured on the semi-crystalline PET and the amorphous PS samples. The phase transition temperatures measured are plotted in Figure 5 as a function of those measured by DSC.

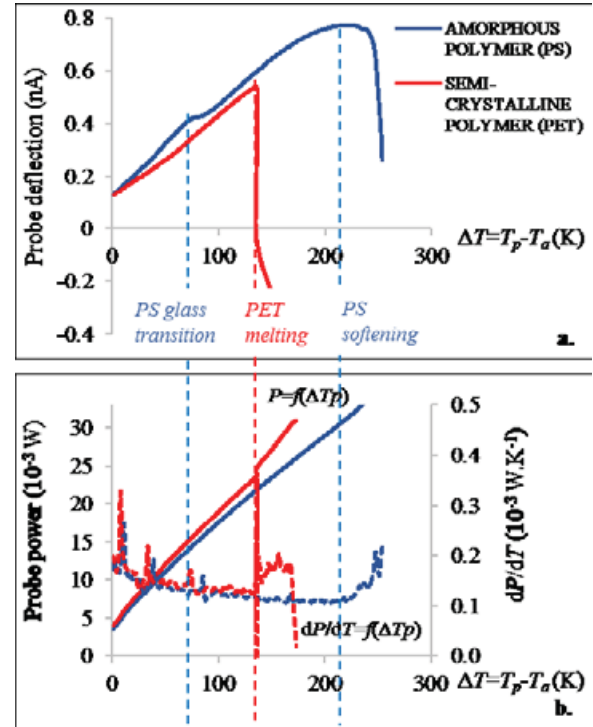


Figure 4: Measurements for PS and PET samples as a function of $\Delta T = (T_p - T_a)$: (a) thermomechanical data and (b) power P and global thermal conductance dP/dT_p .

From the results of thermomechanical and thermal measurements of reference polymeric materials we deduce the following.

(i) Thermomechanical analysis using SThM can be used in the temperature range $[20-300^\circ\text{C}]$ to detect both the glass transition and the softening of amorphous polymers, and the melting of semi-crystalline polymers for phase transition (see Figure 4.a for the PS and PET samples). As shown in Figure 5 the temperatures T_p determined from the electrical resistance calibration in the oven at which these phase changes occur are below the reference temperatures measured by DSC (up to 22 % relative difference). This difference can be mainly ascribed to the temperature calibration of the probe in the oven, as the probe is isothermal in this case while it is not when operated for measurements. In Section 4 a discussion on other sources of uncertainty linked to the measurement method will be performed.

(ii) A variation of the global thermal conductance of the probe-sample system $G_{tot} = dP/dT$ can be observed at the melting or softening of the studied polymers (see two examples in Figure 4b for the PET and PS samples). This takes place mostly because the probe-sample contact area increases as the probe sinks into the polymer in the "liquid" zone (after melting or softening).

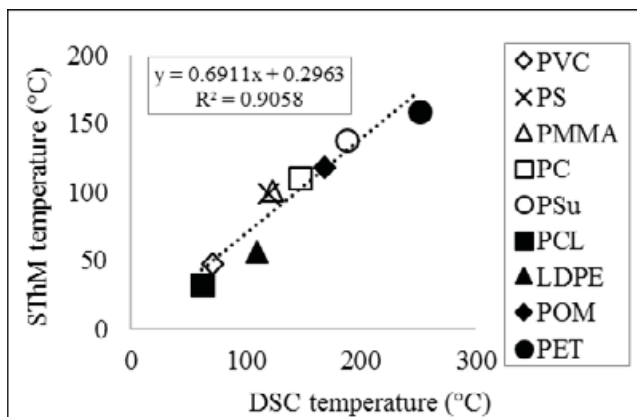


Figure 5: Phase change temperatures measured using SThM versus those measured using DSC.

As a conclusion, all the critical temperatures can be detected and thermal conductivity can be determined as a function of probe temperature. Applying a relationship of correspondence between the probe temperature, being calibrated in an oven, and T_g , T_m and T_s DSC measurements leads to a relative uncertainty of up to 22 %, which is reduced by considering the temperature field inside the probe. The determination of the real contact area between the probe and the sample, either in the solid or in the liquid state, could further improve the sensitivity of scanning thermal microscopy with the doped silicon probe.

4. Uncertainty analysis and measurement inter-laboratory comparison results

4.1 Protocol for measurement and blind comparisons

The procedure used for the uncertainty analysis basically follows the experimental steps suggested by Anasys Instruments [3,4]. For the inter-laboratory comparison we used the following procedure. Calibration and measurements were performed under ambient air conditions (air at temperature = 23 °C and RH = 50 %) and for a current ramp of 0.1 V.s⁻¹. The three devices were characterized and calibrated by using the four semi-crystalline samples spanning T_m up to 250 °C (Table 1) and the silicon sample, and by performing probe deflection measurements as a function of the voltage applied to the probe (heating voltage) while the probe is free in air (no contact with a sample). At least five repeated measurements were performed over a temperature range starting at a temperature below the transition temperature and finishing at a temperature above the transition temperature for every sample. The calibration was performed before and after the measurements of the test samples (amorphous polymers in Table 1). All the samples were measured with one and only probe per operator or per compared measurement series.

4.2 Uncertainty analysis

There are numerous potential uncertainty contributions related both to calibration of the probe temperature scale and

to the thermomechanical response of the samples. Here we briefly discuss different effects participating in the measurement and suggest the procedure to estimate their magnitude and contribution to the final uncertainty.

An important aspect of the uncertainty analysis is that the temperature scale is calibrated using the same method like the measurements on the unknown samples. This helps in reducing many of the potential uncertainty sources related to the thermomechanical response, as discussed below, however it adds extra uncertainties related to the temperature scale calibration. In contrast to the calibration in an oven (as performed in the previous Section), where many different temperatures can be measured, the phase-transition temperature calibration with a limited number of samples leads to a calibration with only few points (in our case four points) and we need to interpolate between them. The following uncertainty sources were also identified:

- *Probe electrical resistance instability:* the probe temperature is obtained from its electrical resistance; however this resistance can change during the experiment (due to either to a slow drift out or a sudden jump). This can have several reasons but one of the major effects is related to the laser spot position on the cantilever. By photoelectric effect, the laser produces some extra voltage to the circuit, which highly depends on position of the laser spot on the cantilever. When the probe gets heated, it expands and slightly deflects. This effect itself slightly change the position of the laser spot with respect of the cantilever. Moreover, after heating the probe repeatedly, there can be some residual deformation, leading to systematic shift of the resistance.
- *Uncertainty related to the calibration curve fitting:* Typically, the calibration data are fitted using linear or quadratic dependence [3]. The number of calibration samples is usually low (sometimes the same as the number of free parameters in the fit), so it is hard to get the uncertainty via fitting. As an alternative, we can compare the fitting results from the calibration data measured before and after measurements on the unknown samples. This includes even more uncertainty aspects than only fitting procedure would allow.
- *Uncertainty of the reference values of the calibration samples:* This is related to both the measurements with DSC and the fact that the thermal conductivities of the reference samples and samples to be measured do not have the same thermal conductivity (effusivities) [4]. Therefore, the thermal balance of the probe-sample system depends on the thermal conductivity also and affects the probe temperature at the sample phase transition. While certainly significant, the second effect is neglected in what follows according to the Anasys procedure.

Even if the procedure for system calibration reduces the uncertainties related to the thermomechanical response, there are still some effects to be discussed:

- *Apparent vertical deflection observed when a DS probe is heated.*

- *Uncertainty related to the drift of the deflection signal* after switching the feedback off and prior to starting the current ramp.
- *Uncertainty related to changes of the shape of deflection vs. heating voltage curve:* For a probe free in air and measurement on Si sample this is mostly related to the probe deformation while heated and ideally should be the same for calibration samples and unknown samples measurement (so it does not contribute to the uncertainty). This is not the case. Two different effects were seen in different experiments; change of the slope on a monotonic curve and complex non-monotonic shape of the curve.
- *Uncertainty related to the difficulty to identify accurately the heating voltage where the phase change occurs*
- *Electronics readout noise.*

In order to estimate and combine all the effects we used available experimental data and Monte Carlo uncertainty analysis approach. The full uncertainty calculation was performed for Device 1 (see Table 2) that provided also estimates for minor uncertainty components that were then used within experimental data evaluation for all the instruments. Main identified uncertainty components were evaluated for each measurement individually. The following experimental data were used for the uncertainty estimation:

- Difference of the calibration curve obtained prior and after measurement on unknown samples. Within Monte Carlo procedure this is added as variance of the calibration factor, together with the uncertainty of reference values as provided in Table 1.
- Slope of deflection vs. heating voltage curve when measured in air and on silicon surface before and after the measurements. Slope or shape of curve changes were taken into account by adding distortion to the curves generated in Monte Carlo procedure. Change of the slope on a monotonic curve and complex non-monotonic shape of the curve were treated as uncertainty input as not enough information was available to treat it as systematic error (and correct it).
- Variance of slopes of the deflection signal after switching the feedback off and prior to starting the ramp. The drift is typically neglected, however as it changes the slope of the curve it can have impact on the maximum position, so it is another slope variance added in the Monte Carlo procedure.
- Electronics readout noise for steady signal. This effect was evaluated directly from the raw data obtained by the electronics before starting the ramp.
- Apart of these inputs that can be deduced from experiments we also added extra terms related to long time observations, like the electronics and quadrant diode signal drift, however these have minor impact on the result.

The Monte Carlo uncertainty calculation started by using ideal curves obtained by averaging multiple experimental curves and smoothing them. Then, the curve shape was altered using the abovementioned criteria; curve maxima for individual altered curves were found to get calibration data.

The reference values for the calibration data construction were altered on basis of the known uncertainty. The procedure was then following the real data evaluation steps - calibration curve was constructed, ideal curves obtained on unknown samples were altered using the same methods as described above, calibrated by the calibration curve and resulting transition temperatures were found and statistically evaluated. More than 1000 curves were simulated for every single measurement (typically much more than what can be reached in experiments). The resulting uncertainty was between 3-5 K depending on transition temperature value and curve shape (flatness of the maximum). The calibration curve nonlinearity and difference of the calibration curve prior and after the measurements was found to be by far the strongest contribution, easily covering all the minor aspects. Consequently, it was found that this remains the major contribution to the final uncertainty: about 50 % for low transition temperatures up to 70 % for high transition temperatures. It was followed by curve slope variance and reference samples uncertainty, around 15 %. The effect of mechanical drift after switching the feedback off was small - 2.5% of the uncertainty - and electronics noise effect was almost negligible - up to 0.2% of the uncertainty. The uncertainty analysis results (expanded uncertainty) were used for error bars shown in graphs in the next section.

4.3 Results and discussion

Figures 6 and 7 show the results of all the measurements for the calibration and the evaluation of the techniques. All data were evaluated in the same way using simple custom-built software, except data labelled "Device 3 Anasys SW" curves where the automated data evaluation in the microscope software was performed to explore the potential differences. The following data sets are therefore shown:

- Device 1 data measured using 300 μm long cantilever (probe 1)
- Device 1 data measured using 200 μm long cantilever (probe 2)
- Device 2 data measured using 200 μm long cantilever
- Device 3 data measured using 200 μm long cantilever, evaluated the same way as the above ones
- the same Device 3 data evaluated using the built-in Anasys software.

The order of samples measured can vary depending on the operator but we have not clearly seen some dependence to this parameter.

Figure 6 shows the calibration data in terms of melting phase-transition temperatures T_m values measured using SThM as a function of the T_m values measured using DSC. These data were obtained prior (cal1) and after (cal2) measurements on the test samples. In the calibration step, heating voltage data were averaged for each probe/device combination and a linear fit was used to translate the heating voltage values measured on the calibration samples into temperatures. In this way all the data sets were calibrated. Calibration results obtained by the different devices look very similar, having a similar S shape. This justifies that calibration data cannot be

fitted by a quadratic curve in the calibration step. As higher-order fits are not possible because of the limited number of calibration samples, it was chosen to fit the experimental data by means of a linear curve prior to the evaluation. For a given sample the maximum difference between temperatures measured with SThM devices is about 20 K and the maximum deviation obtained between SThM data and reference temperature is about 22 K.

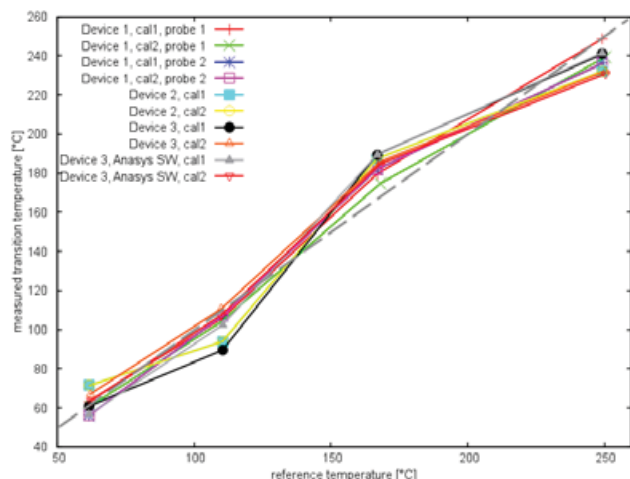


Figure 6: All the calibration data, independently plotted for data obtained prior (cal1) and after (cal2) measurements. Data are already converted to temperature to be mutually comparable and to show the typical calibration curve shape. The dashed line is the linear fit.

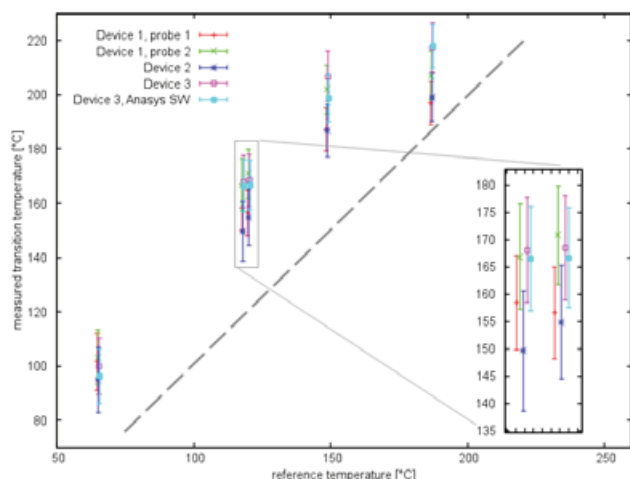


Figure 7: Results on the five test samples (Table 3), including different probes and different evaluation methods. Error bars are showing the expanded uncertainty ($k = 2$). Points are slightly mutually shifted in the x-axis direction for better visibility.

Figure 7 provides the SThM measurements on the amorphous test samples as a function of the glass-transition temperature T_g reference values. The values of temperature measured using SThM are larger than those obtained by DSC whatever the device used. For a given sample, the maximum difference between temperatures measured with SThM devices is about 22 K, which is of the same order of magnitude than in the

calibration step, and the difference of temperature between SThM data and DSC measurements varies from 25 to 40 K, which is larger than in the calibration step.

Within the calculated uncertainties the results are in agreement, however uncertainty is much higher than originally expected. Linearity and repeatability of data calibration is the main source of uncertainty. This can be related to probe changes, as part of it is related to probe changes (observed by measurements in air and on silicon), so novel and better probes would be useful. However the main part of it remains unknown. Linearity of calibration curve could be improved by better choice of samples, however the repeatability (drift of calibration coefficients) remains problematic and this already adds few kelvins to the uncertainty. This effect could be related to probe contamination which, after approximately 50 indentations into various plastics, could be significant. It is suggested that the probe can be cleaned by heating it up, however this changes the electrical properties, so this cannot be used within single experiment where we need the data to be mutually consistent. The considered probe geometry (cantilever length), used electronics and curve maximum search procedure have no impact on the result (within the large uncertainty).

On basis of these measurements the suggested measurement protocols were improved by adding second calibration set measurements after unknown samples measurement. It would be good to measure also the drift, which is not possible for commercial devices (but can be done manually). Also the checks on air and silicon are important to eliminate potential uncertainty related to probe properties change. Probe calibration in oven could be considered not useful as the probe resistance depends highly on the laser position on the cantilever, therefore it is also not recommended to remove or realign the probe during the experiment - all the data should be measured under exactly same conditions and with exactly same probe.

Acknowledgements

The research leading to these results has received funding from the EU FP7 Programme under GA n°604668.

Literature

- [1] S. Gomès, A. Assy and P.O. Chapuis, "Scanning thermal microscopy: a review", PSSa 212, 3, 2015, pp.477-494.
- [2] QUANTIHEAT Application note "Reference samples for phase change temperature measurement and for thermal conductivity measurement", refer to <http://www.quantitheat.eu/> 2017.
- [3] www.anasysinstruments.com
- [4] W. P. King, B. Bhatia, J. R. Felts, H. J. Kim, B. Kwon, B. Lee, S. Somnath and M. Rosenberger, "Heated afm cantilevers and their applications", Annu. Rev. Heat Transf. 16, 16, 2013, pp; 287-326.